Journal of Thermal Biology 84 (2019) 426–430

Contents lists available at ScienceDirect

Journal of Thermal Biology

journal homepage: www.elsevier.com/locate/jtherbio

Characterization of ice recrystallization inhibition activity in the novel freeze-responsive protein Fr10 from freeze-tolerant wood frogs, *Rana sylvatica*

Dung Le Tri[a], Christine L. Childers[a], Madeleine K. Adam[b], Robert N. Ben[b], Kenneth B. Storey[a], Kyle K. Biggar[a,*]

[a] Institute of Biochemistry and Department of Biology, Carleton University, 1125 Colonel By Dr., Ottawa, ON, K1S 5B6, Canada
[b] Department of Chemistry and Biomolecular Sciences, University of Ottawa, 10 Marie Curie Dr., Ottawa ON, K1N 6N5, Canada

ARTICLE INFO

Keywords:
Fr10
Thermal shift assay
Rana sylvatica
Freeze tolerance
Ice recrystallization

ABSTRACT

Fr10 is a secreted freeze-responsive protein found in the wood frog (*Rana sylvatica*). This protein has gained notable research attention for its highly dynamic expression in response to seasonal freezing stress, while its over-expression has been documented to enhance freeze tolerance in cold-susceptible cultured cells. This study further characterizes the properties of this novel protein with regards to thermal stability and ice recrystallization inhibition (i.e. IRI) activity. Thermal stability was assessed using differential scanning fluorimetry, with an experimental T_m value of 50.8 ± 0.1 °C. Potential IRI activity of Fr10 was evaluated using a recently developed nanoparticle-based colorimetric assay, where Fr10 displayed the ability to prevent freeze-induced aggregation of gold nanoparticles. Based upon this assay, Fr10 protein appeared to have a low level of IRI activity and it was therefore predicted that one of Fr10's biological functions may be to inhibit ice crystal growth via recrystallization. A SPLAT cooling assay was then employed to directly characterize the IRI properties of Fr10 and provide further insight into this hypothesis. In the presence of 30 μM of Fr10, a 40% reduction in the mean grain size of ice crystals relative to the control samples was observed, thus introducing the possibility of Fr10 to inhibit ice recrystallization. Collectively, the results from this study provide new insight into the potential of further exploring the potential of this vertebrate freeze-responsive protein in cryoprotection.

1. Introduction

Cryopreservation is crucial to various medical, research and industrial applications, such as in food storage, preservation of living tissues for transplant, cryosurgery, etc. Nevertheless, freezing-induced damage poses a major challenge to this process, mainly due to the phenomenon of ice recrystallization, in which water molecules are transferred from smaller ice crystals to promote the nucleation and growth of larger ones (i.e., recrystallization) (Capicciotti et al., 2013; Duman, 2015). Recrystallization is responsible for the decreased quality of frozen foods, as well as irreversible cellular damage that result in reduced viability of cryopreserved cells and living tissues (Capicciotti et al., 2013). As a result, the use of cryoprotective agents is necessary to prevent freezing-induced damage in cryopreservation. In recent years, major interest has been directed towards investigating biological cryoprotectants. This includes various proteins and glycoproteins found in cold-tolerant bacteria, fish and insects. These biological cryoprotectants exhibit remarkable cryoprotective capabilities at very low working concentrations, while also having little to no toxicity, thereby being much more favorable in cryopreservation applications compared to currently employed industrial compounds (Duman, 2015; Kim et al., 2017).

Freeze-responsive protein 10 (Fr10) is a freeze-responsive protein discovered through the screening of cDNA from the liver of frozen wood frogs (*Rana sylvatica*). The Fr10 protein is only found in the freeze-tolerant wood frog and has a chain length of 90 amino acids and a molecular weight of 10 kDa (Cai and Storey, 1997). Given its highly dynamic over-expression in response to seasonal winter freezing, this protein has been previously hypothesized to play a role in the wood frog's ability to tolerate and survive low temperature (down to −16 °C) (Costanzo et al., 1993, 2013; Storey and Storey, 1988, 1992; Storey, 2004). Results from previous studies of freeze-tolerance in the wood frog have also proposed that an overexpression of this protein is crucial to the frog's survival at freezing conditions (Storey, 2004). A subsequent

* Corresponding author.
E-mail address: kyle_biggar@carleton.ca (K.K. Biggar).

https://doi.org/10.1016/j.jtherbio.2019.07.030
Received 25 January 2019; Received in revised form 9 July 2019; Accepted 27 July 2019
Available online 29 July 2019
0306-4565/

study also demonstrated that freeze-intolerant silkworm cell lines transfected with the Fr10 gene exhibited greater survival capacity after 1 h freezing at temperatures as low as −6 °C; a temperature that proved detrimental to cells only containing the host vector (Biggar et al., 2013). As a result, this protein has demonstrated potential for its study as a general bio-cryoprotectant.

Although the frog also produces massive amounts of glucose inside the cells to regulate the osmotic removal of water from cytoplasm (Costanzo et al., 1993), studies of Fr10-transfected silkworm cell lines showed that these cells survived freezing as long as they produced Fr10 protein. Given that the transfected cells did not increase glucose levels in response to freezing, these results suggested that Fr10 alone is a significant component in preventing freezing-induced cellular damage (Biggar et al., 2013). It was also reported that Fr10 is found in extracellular quantities in both wood frog and Fr10-transfected silkworm cells in response to freezing (Biggar et al., 2013; Storey, 2004). This suggests that Fr10 protein may be deposited extracellularly, where it may carry out a still unknown function (Biggar et al., 2013; Duman, 2015). One hypothesized general function for Fr10 could include a role as a potential ice-binding protein (IBP). IBPs can mitigate freezing-induced cellular damage through several mechanisms: (1) thermal hysteresis (TH), (2) ice recrystallization inhibition (IRI), and (3) ice nucleation control (this includes dynamic ice binding (DIS)), with most IBPs exhibiting more than one of these activities (Duman, 2015; Mitchell et al., 2015). IBPs with high TH activity (commonly found in freeze-avoiding species, where they prevent organismal freezing) are considered true antifreeze proteins (AFPs). By contrast, IBPs in freeze-tolerant species are mostly low-TH IBPs, which exhibit significantly lower TH and instead rely mostly on IRI activity to prevent ice crystal growth through recrystallization; acting to prevent damage to cellular structure (Duman, 2015; Mitchell et al., 2015). As Fr10 is expressed in the freeze-tolerant *R. sylvatica*, it is speculated that this protein would primarily exhibit IRI activity, while likely conferring minimal TH (Duman, 2015). IRI activity of IBPs is currently of interest in cryoprotection research, due to the aforementioned association of ice recrystallization with freezing-induced damage to cellular structures and thus irreversible destruction of cryopreserved tissues following thawing (Capicciotti et al., 2016; Duman, 2015). The primary objective of this study was to document potential IRI activities of Fr10, with such findings providing valuable insight into the function of this novel protein.

2. Materials and methods

2.1. Construct assembly and protein purification

A poly-His tagged Fr10 encoding gene was ligated into pETM11 vectors. The N-terminal 6xHis-tag was separated from the Fr10 protein with an encoded TEV-site for future cleavage and tag removal. Ligated plasmids were amplified and purified from DH5α bacteria. The purified plasmid was then used to transform BL21 bacteria for protein expression using Kanamycin resistance for antibiotic selection.

Cultures were incubated at 37 °C until OD_{600} reached 0.4, and cells were induced with 50 mM isopropyl β-D-1-thiogalactopyranoside. Incubation at the same temperature continued overnight, and cells were then collected following centrifugation at 5000 × *g* for 10 min. The cell pellet was then resuspended with 10 ml of phosphate buffered saline (PBS) buffer and stored at −80 °C. 6xHis-Fr10 protein was then purified by thawing the cell pellet and adding 0.1% v/v of E64, Bestatin and Pepstatin, 1% v/v PMSF, 10% v/v of Triton X-100, 1 mg/mL Lysozyme, 50U of Benzonase. Cells were then sonicated for 20 s on/off for a total of 5 cycles on ice. The lysate was then incubated for 1 h at 37 °C on a rocking platform, and then centrifuged at 12,000 × *g* for 30 min. The supernatant containing soluble protein was then removed and the 6xHis-Fr10 protein was purified using Ni^{2+}-NTA affinity purification. Fr10 was then eluted from the affinity column using 5 mL of 250 mM imidazole and collected in 10 × 0.5 mL fractions and tag removed.

Protein concentration was determined using the Bio-Rad protein concentration assay (modified Bradford assay; BioRad Cat# 5000006) at 595 nm. The concentration of protein was calculated from the average absorbance against a standard curve generated using bovine serum albumin (BSA). Protein purity was assessed by running the collected fractions on a 15% polyacrylamide gel using SDS-PAGE. The gel was run at 125 mV for 50 min in Tris-Glycine running buffer. The gel was then stained for total protein using Coomassie Blue R-250 and protein molecular weights were determined based on relative migration compared to the BLUeye prestained protein ladder (FroggaBio, Cat#PM007). Protein purity was based on densitometry of Coomassie-stained proteins following SDS-PAGE and was determined by the fraction of Fr10 densitometry values to total stained protein.

2.2. T_m prediction and differential scanning fluorimetry (DSF)

For DSF experiments, samples contained 12.5 µL of either PBS (control; buffer only) or Fr10 protein (0.01 µg/µL in PBS). Each well also contained 7.5 µL of 40× SYPRO orange dye (in PBS) for a total reaction volume of 20 µL. The thermocycler was set to increase temperatures from 15 °C to 95.0 °C at 0.5 °C increments and to collect fluorescence for 15 s at each temperature step to monitor any change in SYPRO orange emission. The negative rate of change in fluorescent activity over time was monitored and used to identify the melting temperature (T_m) of Fr10 as previously described (Vivoli et al., 2014).

2.3. Nanoparticle-based aggregation assay

The ability of Fr10 to mitigate freeze-induced damage was tested through its ability to protect gold nanoparticle aggregation during freezing. First, aggregation of nanoparticles was determined in the presence of other compounds with known activity as controls, including polyvinyl alcohol (PVA; positive control), polyethylene glycol (PEG; negative control) and bovine serum albumin (BSA; protein negative control with weak *in vitro* IRI activity). PVA and PEG were made in a concentration range between 0 and 5.0 mg/ml while the protein samples of BSA and recombinant Fr10 were prepared with concentrations ranging between 0 and 0.025 mg/ml, all in a flat-bottom transparent 96-well microplate. A total of 50 µL of gold nanoparticles (AuNP) (30 nm stabilized particles; Cyto Diagnostics, Cat# CG-134 30-20) were added to each well to a total volume of 100 µL. All sample preparation was done at 4 °C. The absorbance of the samples was measured at 520 nm after 4 h of freezing at −20 °C and 45 min thawing at room temperature (RT) as previously described (Mitchell et al., 2015). The peak absorbance at 520 nm was subtracted by the calculated value of absorbance at 520 nm using the slope of the regression line obtained using the fluorescence values at 450 and 680 nm. The difference between the peak and the regression line was used to plot the nanoparticle protection capacity for each small molecule or protein. Results were followed up by an unpaired *t*-test to statistically determine differences between Fr10 and BSA.

2.4. SPLAT cooling assay

The IRI activity was measured in triplicate using the SPLAT cooling assay (Ali and Wharton, 2016; Mitchell et al., 2015; Wharton et al., 2007). A 10 µL drop of sample (at RT) was dropped (pipette equipped with low retention tips) 2 m above a polished aluminum block that had been previously cooled to −80 °C with dry ice. The droplet immediately froze upon contact with the surface of the block, creating a wafer approximately 1 cm in diameter and 20 µm thick. The wafer was separated from the surface of the aluminum block using pre-cooled tools and transferred to a cryostage maintained at −6.4 °C. The wafer annealed for 5 min at −6.4 °C and was then photographed between crossed polarizing filters (Nikon CoolPix 5000). One image was selected

from each wafer for analysis. Ice crystals with well-defined boundaries within the image were outlined using ImageJ software. The ice crystal areas were averaged, and the ice crystal mean grain size (MGS) of the sample was compared to the MGS of the PBS positive control for recrystallization for the same day of testing.

3. Results and discussion

Many IBPs, which include AFPs, antifreeze glycoproteins (AFGPs) and low TH-IBPs, exhibit potent IRI activity and thus can prevent freezing-induced damage to living tissues when subjected to freezing temperatures (Capicciotti et al., 2013; Duman, 2015). While the exact mechanism of IRI activity has not been fully elucidated, it is proposed to result from inhibition of water transfer between the ice crystals and liquid water; preventing the growth of larger ice crystals through recrystallization. This may either involve binding of the IBP to the surface of ice crystals to prevent their growth, or through a disruption of the hydrogen bonding network in liquid water. The latter renders the transfer of water molecules between ice crystals and liquid water energetically unfavorable (Capicciotti et al., 2013).

Compared to industrial cryoprotectants like ethylene glycol or dimethyl sulfoxide (DMSO), IBPs can prolong tissue viability at significantly lower concentrations and with little to no toxicity, making their use as a cryoprotectant particularly intriguing (Duman, 2015; Kim et al., 2017). The novel freeze-responsive protein Fr10, is currently of interest for its usefulness in cryopreservation. Previous studies have demonstrated that Fr10-transfected silkworm cells showed higher survival rate post-thawing compared to untransfected counterparts (Biggar et al., 2013), although the exact mechanism of action of this protein had not been fully explored. It has been previously proposed that Fr10 may exhibit similar freeze-responsive mechanisms as LS-12, a type-IV AFP isolated from the longhorn sculpin (*Myoxocephalus octodecemspinosus*), due to their great structural homology in terms of size (72 and 108 amino acids, respectively), alanine content (9.7% and 11%, respectively), Glu/Gln content (22% and 26%, respectively), and their predicted structures (a four α-helical antiparallel bundle) (Biggar et al., 2013; Deng et al., 1997; Duman, 2015; Storey and Storey, 2017). Since LS-12 has been previously shown to exhibit both TH and ice shaping activities (required some degree of ice binding capability), we originally posited the possibility that Fr10 could also exhibit ice-binding properties (specifically, IRI activity) mediated by its predicted helical bundle structure (Deng et al., 1997; Deng and Laursen, 1998; Gauthier et al., 2008). Therefore, this study aimed to characterize potential IRI activity and thermal stability of the Fr10 protein *in vitro*, both of which may prove insightful in understanding its potential in cryoprotective applications (Biggar et al., 2013; Bischof and He, 2005; Nowshari and Brem, 1998).

The recombinant Fr10 protein was successfully purified and the molecular weight was confirmed to be approximately 10 kDa through SDS-PAGE (Fig. 1). Following the successful recovery of recombinant Fr10 protein, DSF was employed to assess the thermal properties of Fr10 by determining its temperature of denaturation (T_m) (i.e., the temperature at which an equilibrium between the biologically active native protein and its unfolded form is established). Results indicated a T_m of 50.8 ± 0.1 °C for Fr10 (Fig. 2). Comparatively, two ice-binding proteins (IBPs) derived from the Antarctic bacteria of the *Flavobacteriaceae* family and *Euplotes focardii* consortium, were previously found to have a T_m at 53.5 °C and 66.4 °C, respectively (Mangiagalli et al., 2016; Wang et al., 2017). By contrast, a type-III AFP isolated from Arctic eel pout (*Macrozoarces americanus*) was reported to have a T_m value of approx. 46 °C. Fr10 therefore exhibited a similar T_m value to other known AFPs and IBPs in other species.

To assess IRI activity *in vitro* we used a recently developed gold nanoparticle (AuNP) assay (Mitchell et al., 2015). As recrystallization occurs, gold nanoparticles are excluded from the ice crystals along with other solutes, leading to their aggregation. In the presence of a molecule with detectable IRI activity, this aggregation caused by recrystallization can be hindered or possibly prevented. By monitoring the change in absorbance of the nanoparticles before and after freezing

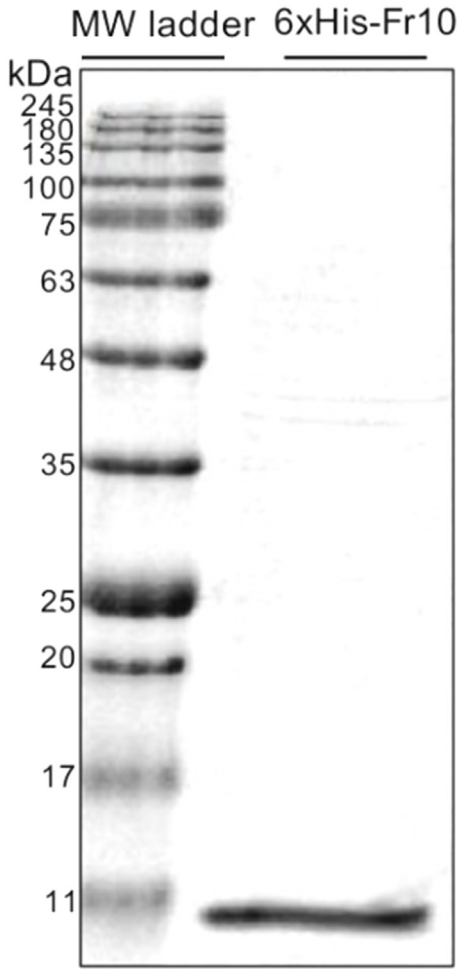

Fig. 1. Fr10 expression and affinity purification. The Fr10 protein was affinity purified by immobilized Ni^{2+}-NTA affinity chromatography.

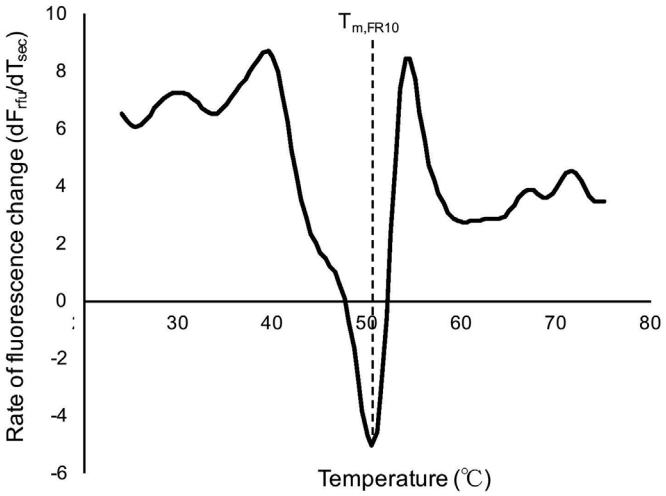

Fig. 2. Thermal stability of Fr10 protein. Differential scanning fluorimetry (DSF) representative melt peak showing the rate of change in fluorescent intensity from Fr10, with the inverted peak indicating the T_m value. The average inflexion point is located at 50.83 ± 0.06 °C. Data was collected using Bio-Rad CFX Connect Real Time System thermal cycler.

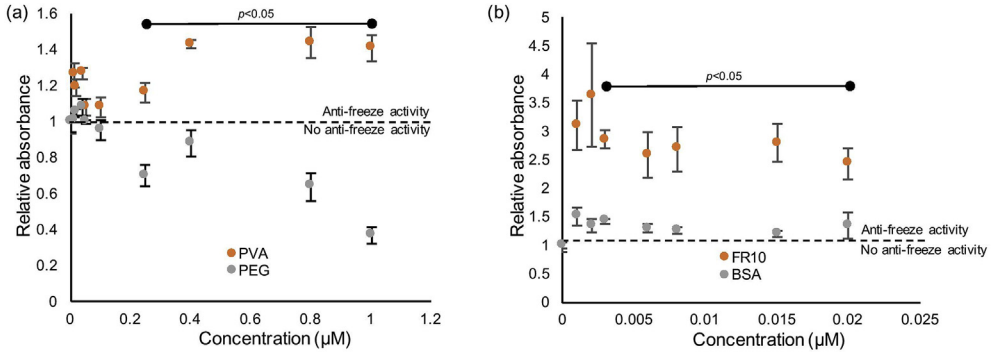

Fig. 3. Gold nanoparticle-based IRI activity assay. (a) Standard curves of polyvinyl alcohol (PVA; positive control) and polyethylene glycol (PEG; negative control), showing the correlation between concentration and relative IRI activity. (b) Experimental curves of Fr10 against BSA protein control, showing the correlation between concentration and IRI activity. Error bars were generated using standard error of each data value. The line going through $y = 1$ marked the borderline between the normalized IRI activity and no IRI activity. Data was collected using BioTek PowerWave HT spectrophotometer. The line of $p < 0.05$ indicated the range at which significant differences between IRI activities were observed, at 95% confidence level between data sets.

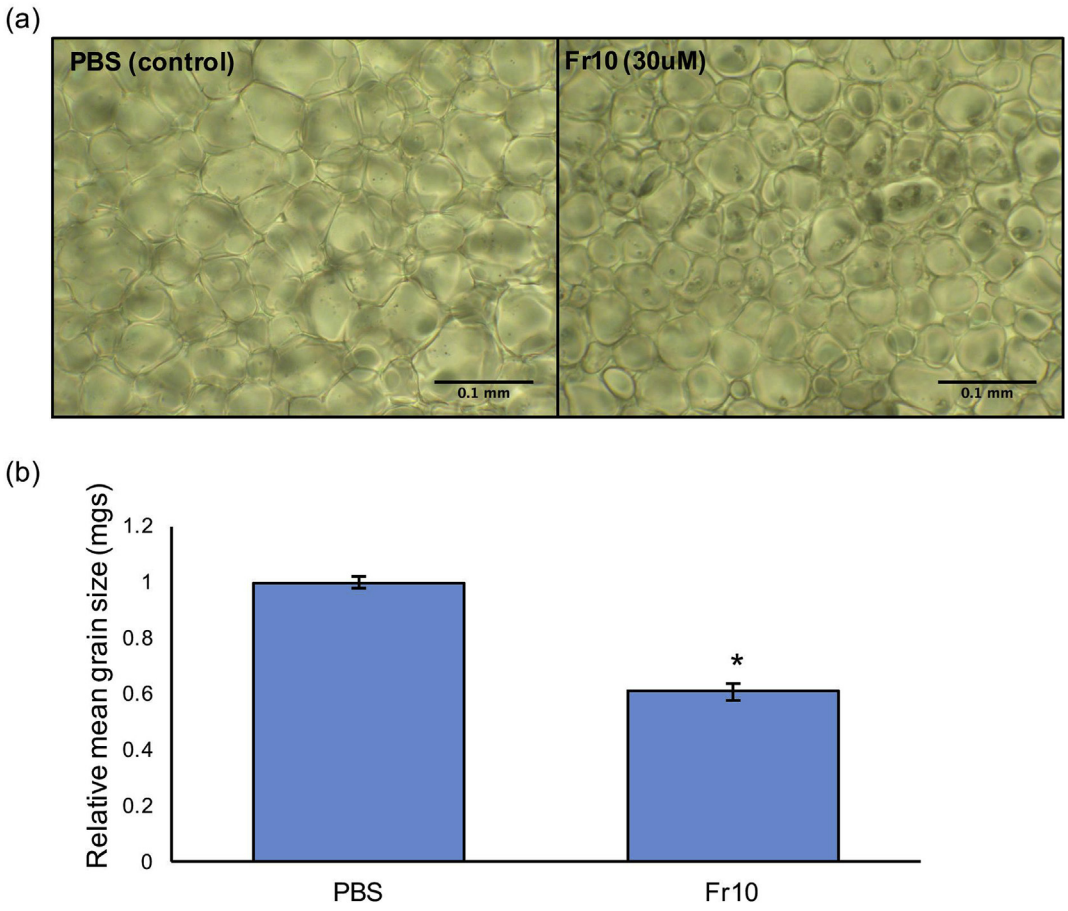

Fig. 4. Ice recrystallization inhibition activity of Fr10 protein from SPLAT cooling assay. (a) Ice crystal images following annealing at −6.4 °C for 5 min in PBS (pH 7.4) (left) and in PBS containing 30 μM Fr10 (right). Both images were taken using Nikon CoolPix 5000 camera fitted onto a compound microscope. (b) Ice recrystallization inhibition analysis of Fr10. The samples (PBS and Fr10) were each performed in triplicate, at an annealing temperature of −6.4 °C for 5 min. PBS sample (control) represents a standard value for relative mean grain size (MGS) of ice crystals. The error bars represent standard error of the mean.

of samples containing Fr10 proteins, the relative IRI properties of Fr10 can be determined based on the degree that it prevents freezing-induced nanoparticle aggregation (Mitchell et al., 2015). In this study, PVA (Mw 30,000–70,000 g/mol) and PEG (Mw 8000 g/mol) were used to generate standard curves that distinguish between the presence and absence of IRI activity, respectively (Mitchell et al., 2015). The IRI property of Fr10 was also tested against BSA (a protein with very weak reported *in vitro* IRI activity) as a protein comparison.

The assay was validated through evaluation of relative IRI activity by polyvinyl alcohol (PVA) and polyethylene glycol (PEG). The overall level of relative IRI activity for PVA and PEG was found to be consistent with the previously reported results obtained by Mitchell and colleagues (Mitchell et al., 2015). PEG samples displayed a lack of IRI activity, while PVA demonstrated concentration-responsive IRI activity (Fig. 3A). Fr10 protein demonstrated greater protection against AuNP aggregation when compared against the weak-IRI control BSA (Fig. 3B). These results indicated that Fr10 has an ~2-fold higher apparent IRI activity compared to BSA protein at the same concentrations when exposed to −20 °C. The saturation of Fr10 apparent IRI activity was reached at 0.001 mg/ml (Fig. 3B). Although these results support some measurable level of IRI activity for Fr10, it should be mentioned that it is unknown at this time if these values are biologically relevant in the frog.

To further explore possible IRI activity for recombinant Fr10

protein, an additional assay to directly detect IRI was used to observe the inhibitory effects on the formation of ice crystals in the presence of each of these controls and Fr10. For this purpose, a SPLAT assay was employed as previously described (Capicciotti et al., 2016; Mitchell et al., 2015; Wharton et al., 2007). The reported annealing temperature (−6.4 °C) is comparable to those previously reported to be the minimum temperature that Fr10 protein could function effectively to protect freeze-intolerant silkworm cells in cell culture (Biggar et al., 2013). The SPLAT cooling assay displayed that the MGS of ice crystals in samples with 0.33 mg/ml (30 μM) of Fr10 (in PBS) protein was approximately 60% of control samples at −6.4 °C (Fig. 4). For comparison, a type-III AFP from ocean pout was reported to have a similar inhibitory concentration in the low μM range, while many AFGPs exhibit IRI activity in the nanomolar ranges (Olijve et al., 2016; Voets, 2017). It is possible that the relatively lower IRI activity observed for Fr10 using the AuNP assay could potentially result from the adsorption of proteins directly to the nanoparticles, which may partially contribute to the prevention of aggregation. Indeed, previous characterization of IRI activity in BSA using the AuNP assay reported that BSA exhibited IRI activity at concentrations as low as 0.5 mg/ml, whereas subsequent validations using SPLAT method showed that BSA only exhibited considerable IRI activity at concentrations above 10 mg/ml – a difference of 20-fold (Mitchell et al., 2015). This could therefore explain the significant difference between the IRI activity reported for Fr10 using two different methods in this study. To fully elucidate the function of Fr10 in the freeze-tolerant wood frog, it will be important to investigate the collective contributions of other freeze-responsive proteins and glycolipid components in the wood frog (Sullivan et al., 2015).

It was not possible to fully determine if Fr10 is a bone fide IBP from its apparent IRI activity, and the ice-binding properties of Fr10 would require experimental validation using ice-affinity chromatography (Marshall et al., 2016). It was also not possible to classify Fr10 as either an AFP or a low-TH IBP based on the findings in this study, since both types can exhibit IRI activity (Duman, 2015). Quantification of potential TH activity conferred by the Fr10 protein is therefore also necessary for its final classification; this can be studied using a nanoliter osmometer (Braslavsky and Drori, 2013) or sonocrystallization (Gaede-Koehler et al., 2012). Additionally, Fr10 may also have alternative biologically relevant functions control ice nucleation, which may include dynamic ice shaping (DIS) or initiation of ice nucleation in the extracellular fluid, as well as osmotic regulation, to promote an ice-free cytosol (no freeze-tolerant vertebrate has been documented to survive intracellular freezing) (Duman, 2015; Storey and Storey, 2017). Investigating these properties of Fr10 can also provide major insights into its application as a cryoprotectant. The study of TH and ice nucleation control properties of Fr10 are nevertheless beyond the scope of this study and will instead be covered by future research to further assess the protein's usefulness in cryoprotective applications.

Collectively, this study has explored the possible IRI activity and thermal stability of Fr10, an extracellular protein with previously documented cryoprotective abilities in cell culture (Biggar et al., 2013). Overall, we have demonstrated that Fr10 displays moderately low IRI activity *in vitro*.

Acknowledgements

This research was funded by Discovery grants from the Natural Sciences and Engineering Research Council of Canada to K.K.B and K.B.S. R.N.B. acknowledges support from NSERC, Canadian Blood Services (CBS), and the Canadian Institutes of Health Research (CIHR). M.K.A. acknowledges NSERC for a Canada Graduate Scholarship (CGS D).

Appendix A. Supplementary data

Supplementary data to this article can be found online at https://doi.org/10.1016/j.jtherbio.2019.07.030.

References

Ali, F., Wharton, D.A., 2016. Ice-active substances from the Infective juveniles of the freeze tolerant entomopathogenic nematode. *Steinernema feltiae*. PLoS One 11.
Biggar, K.K., Kotani, E., Furusawa, K.T., Storey, K.B., 2013. Expression of freeze-responsive proteins, Fr10 and Li16, from freeze-tolerant frogs enhances freezing survival of BmN insect cells. FASEB J. 27, 3376–3383.
Bischof, J.C., He, X., 2005. Thermal stability of proteins. Ann. N. Y. Acad. Sci. 2066, 12–33.
Braslavsky, I., Drori, R., 2013. LabVIEW-operated novel nanoliter osmometer for ice binding protein investigations. J. Vis. Exp. 4189.
Cai, Q., Storey, K.B., 1997. Upregulation of a novel gene by freezing exposure in the freeze-tolerant wood frog (*Rana sylvatica*). Gene 198, 305–312.
Capicciotti, C.J., Malay, D., Ben, R.N., 2013. Ice Recrystallization Inhibitors: from Biological Antifreezes to Small Molecules.
Capicciotti, C.J., Mancini, R.S., Turner, T.R., Koyama, T., Alteen, M.G., Doshi, M., Inada, T., Acker, J.P., Ben, R.N., 2016. *O*-Aryl-Glycoside ice recrystallization inhibitors as novel cryoprotectants: a structure–function study. ACS Omega 1, 656–662.
Costanzo, J.P., Lee, J.R., Lortz, P.H., 1993. Glucose concentration regulates freeze tolerance in the wood frog *Rana sylvatica*. J. Exp. Biol. 181, 245–255.
Costanzo, J.P., do Amaral, M.C.F., Rosendale, A.J., Lee Jr., R.E., 2013. Hibernation physiology, freezing adaptation and extreme freeze tolerance in a northern population of the wood frog. J. Exp. Biol. 216, 3461–3473.
Deng, G., Laursen, R.A., 1998. Isolation and characterization of an antifreeze from the longhorn sculpin, *Myoxocephalus octodecimspinosus*. Biochim. Biophys. Acta. 1388, 305–314.
Deng, G., Andrews, D.W., Laursen, R.A., 1997. Amino acid sequence of a new type of antifreeze protein, from the longhorn sculpin *Myoxocephalus octodecimspinosis*. FEBS Lett. 402, 17–20.
Duman, J.G., 2015. Animal ice-binding (antifreeze) proteins and glycolipids: an overview with emphasis on physiological function. J. Exp. Biol. 218, 1846–1855.
Gaede-Koehler, A., Kreider, A., Canfield, P., Kleemeier, M., Grunwald, I., 2012. Direct measurement of the thermal hysteresis of antifreeze proteins (AFPs) using sonocrystallization. Anal. Chem. 84, 10229–10235.
Gauthier, S.Y., Scotter, A.J., Lin, F.H., Baardsnes, J., Fletcher, G.L., Davies, P.L., 2008. A re-evaluation of the role of type IV antifreeze protein. Cryobiology 57, 292–296.
Kim, H.J., Lee, J.H., Hur, Y.B., Lee, C.W., Sun-Ha, Park, Bon-Won, Koo, 2017. Marine antifreeze proteins: structure, function, and application to cryopreservation as a potential cryoprotectant. Mar. Drugs 15, 1–27.
Mangiagalli, M., Bar-Dolev, M., Tedesco, P., Natalello, A., Kaleda, A., Brocca, S., de Pascale, D., Pucciarelli, S., Braslavsky, I., Lotti, M., 2016. Cryo-protective effect of an ice-binding protein derived from antarctic bacteria. FEBS J. 284, 163–177.
Marshall, C.J., Basu, K., Davies, P.L., 2016. Ice-shell purification of ice-binding proteins. Cryobiology 72, 258–263.
Mitchell, D.E., Congdon, T., Rodger, A., Gibson, M.I., 2015. Gold nanoparticle aggregation as a probe of antifreeze (glyco) protein-inspired ice recrystallization inhibition and identification of new IRI active macromolecules. Sci. Rep. 5, 15716.
Nowshari, M.A., Brem, G., 1998. Effect of cryoprotectants and their concentration on post-thaw survival and development of expanded mouse blastocysts frozen by a simple rapid-freezing procedure. Theriogenology 50, 1001–1013.
Olijve, L.L., Vrielink, A.S.O., Voets, I.K., 2016. A simple and quantitative method to evaluate ice recrystallization kinetics using the circle. Hough Transform Algorithm 16, 4190–4195.
Storey, K.B., 2004. Strategies for exploration of freeze responsive gene expression: advances in vertebrate freeze tolerance. Cryobiology 48, 134–145.
Storey, K.B., Storey, J.M., 1988. Freeze tolerance in animals. Physiol. Rev. 68, 27–84.
Storey, K.B., Storey, J.M., 1992. Natural freeze tolerance in ectothermic vertebrates. Annu. Rev. Physiol. 54, 619–637.
Storey, K.B., Storey, J.M., 2017. Molecular physiology of freeze tolerance in vertebrates. Physiol. Rev. 623, 665.
Sullivan, K.J., Biggar, K.K., Storey, K.B., 2015. Transcript expression of the freeze responsive gene Fr10 in *Rana sylvatica* during freezing, anoxia, dehydration, and development. Mol. Cell. Biochem. 399, 17–25.
Vivoli, M., Novak, H.R., Littlechild, J.A., Harmer, N.J., 2014. Determination of protein-ligand interactions using differential scanning fluorimetry. J. Vis. Exp. 1, 12.
Voets, I.K., 2017. From ice-binding proteins to bio-inspired antifreeze materials. Soft Matter 13, 4808–4823.
Wang, C., Pakhomova, S., Newcomer, M.E., Christner, B.C., Luo, B.H., 2017. Structural basis of antifreeze activity of a bacterial multi-domain antifreeze protein. PLoS One 12, e0187169.
Wharton, D.A., Wilson, P.W., Mutch, J.S., Marshall, C.J., Lim, M., 2007. Recrystallization inhibition assessed by Splat cooling and optical recrystallometry. Cryo Lett. 28, 61–68.